

# Generation of Inflow Conditions in a Reynolds-Averaged Navier–Stokes Closure

Gwang Hoon Rhee\* and Hyung Jin Sung†

Korea Advanced Institute of Science and Technology,  
Taejon 305-701, Republic of Korea

## Introduction

**M**OST of inflow conditions in a Reynolds-averaged Navier–Stokes (RANS) closure are provided by employing experimental data at a location of the inlet section. An alternative approach for generating turbulent inflow conditions is the separate simulation, which is an auxiliary inflow simulation. Whereas this approach can provide an accurate inflow condition, it requires additional computation time and data storage.<sup>1</sup> Moreover, the drawback of this approach is that it cannot predict the flow accurately when other external terms exist, for example, pressure gradient, buoyancy, etc. Because of consideration of these effects, difficulties are encountered in generating the accurate inlet conditions. It is desirable to prescribe a turbulent inflow condition at the inflow boundary of the computation domain.

In the present study, a new simple method for generating equilibrium turbulent inflow conditions is proposed when calculations are performed with a RANS closure. The inner layer of the turbulent boundary layer, which is governed by the law of the wall, is composed of the viscous sublayer and logarithmic layer.<sup>2</sup> Coles maintained that the deviations or excess velocity of the outer layer above the logarithmic layer have a wakelike shape when viewed from the freestream.<sup>2</sup> Lund et al.<sup>3</sup> devised a composite profile that is obtained by forming a weighted average of the inner and outer layers. In the present study, the inlet values of  $k$  and  $\varepsilon$  are obtained by solving the  $k$ – $\varepsilon$  equations based on the aforesaid composite velocity profile. Here the  $k$ – $\varepsilon$  equations are a subset of the adopted RANS closure. As a validation, the present method is applied to the flows of a backward-facing step.<sup>4–6</sup> The predicted results are compared with the experimental data.

## Generation of Inflow Conditions

Spalding deduced a single composite formula that covered the entire wall-related region<sup>2</sup>:

$$y^+ = u_{\text{inner}}^+ + e^{-\kappa B} \left\{ e^{-\kappa u_{\text{inner}}^+} - 1 - \kappa u_{\text{inner}}^+ - \left[ (\kappa u_{\text{inner}}^+)^2 \right] / 2 - \left[ (\kappa u_{\text{inner}}^+)^3 \right] / 6 \right\} \quad (1)$$

This expression is an excellent fit to inner-layer data all of the way from the wall to the point where the outer layer begins to rise above the logarithmic curve. In Eq. (1),  $\kappa$  and  $B$  are near-universal constants for turbulent flow ( $\kappa = 0.41$  and  $B = 0.55$ ). The inner variables  $u_{\text{inner}}^+ = U/u_\tau$  and  $y^+ = yu_\tau/\nu$  are employed near the wall region.

Coles noted that the deviations or excess velocity of the outer layer above the logarithmic layer have a wakelike shape when viewed

from the freestream.<sup>2</sup> The overlap and outer layers are expressed as

$$u_{\text{outer}}^+ = (1/\kappa) \ln(y^+) + B + (2\Pi/\kappa) f(y/\delta) \quad (2)$$

The quantity  $\Pi$ , called the Coles wake parameter, is directly related to the nonzero pressure gradient, which is constant at equilibrium flow. The wake function  $f$  is normalized to be zero at the wall and unity at  $y = \delta$ . By integrating Eq. (2) across the boundary layer, we obtain<sup>2</sup>

$$\delta^*/\delta = (1 + \Pi)/\kappa \lambda \quad (3)$$

$$\frac{\theta}{\delta} = \frac{\delta^*}{\delta} - \frac{2 + 3.2\Pi + 1.5\Pi^2}{\kappa^2 \lambda^2} \quad (4)$$

where  $\delta$ ,  $\delta^*$ , and  $\theta$  are the boundary-layer thickness, displacement thickness, and momentum thickness, respectively. The local skin-friction coefficient  $C_f = 2/\lambda^2$  is related to  $\Pi$  and  $Re_\delta = U_\infty \delta/\nu$  by evaluating the wall–wake law [Eq. (2)] at the edge of the boundary layer<sup>2</sup>:

$$U_\infty/u_\tau = \lambda = (1/\kappa) \ln(Re_\delta/\lambda) + B + 2\Pi/\kappa \quad (5)$$

The variables  $\delta$ ,  $\Pi$ , and  $u_\tau$  in Eqs. (1) and (2) are obtained by solving Eqs. (3–5).

A composite profile that is approximately valid over the entire layer is obtained by forming a weighted average of the inner and outer profiles<sup>3</sup>:

$$u^+ = u_{\text{inner}}^+ [1 - W(\eta)] + u_{\text{outer}}^+ W(\eta) \quad (6)$$

The weighting function  $W(\eta)$  is defined as

$$W(\eta) = \frac{1}{2} \left( 1 + \left\{ \tanh \left( \frac{a(\eta - b)}{(1 - 2b)\eta + b} \right) \right\} / \tanh(a) \right) \quad (7)$$

where  $\eta = y/\delta$  is the outer coordinate and  $a$  and  $b$  are constants,  $a = 4$  and  $b = 0.2$ . The weighting function is zero at  $\eta = 0$ , 0.5 at  $\eta = b$ , and unity at  $\eta = 1$  (Ref. 3).

In a RANS closure, the inlet conditions of  $k$  and  $\varepsilon$  are generally given by the formula of Rodi and Scheuerer<sup>7</sup>:

$$k = k_e \left( \frac{U}{U_e} \right)^2, \quad \varepsilon = 0.1k \left( \frac{\partial U}{\partial y} \right) \quad (8)$$

However, in the present study, the inlet values of  $k$  and  $\varepsilon$  are obtained by solving the  $k$ – $\varepsilon$  equations in concert with the composite velocity profile [Eq. (6)]. Here the  $k$ – $\varepsilon$  equations are a subset of the adopted RANS closure. This method is analogous to the a priori test of Parneix et al.,<sup>8</sup> in which the values of  $k$  and  $\varepsilon$  are assessed outside of their full predictive context. For example, if the  $k$ – $\varepsilon$ – $f_\mu$  model is chosen as one of a RANS closure, which is known to give good predictions in turbulent separated and reattaching flows, the  $k$ – $\varepsilon$  equations are expressed as

$$0 = \frac{\partial}{\partial y} \left( \left( \nu + \frac{\nu_t}{\sigma_k} \right) \frac{\partial k}{\partial y} \right) + P_k - \varepsilon \quad (9)$$

$$0 = \frac{\partial}{\partial y} \left( \left( \nu + \frac{\nu_t}{\sigma_\varepsilon} \right) \frac{\partial \varepsilon}{\partial y} \right) + \frac{(C_{\varepsilon 1}^* P_k - C_{\varepsilon 2} f_2 \varepsilon)}{T} + C_1 (1 - f_w) \nu \nu_t \left( \frac{\partial^2 U}{\partial y^2} \right)^2 \quad (10)$$

The coupled equations (9) and (10) are solved based on the mean velocity in Eq. (6). Details regarding the model formulation and model constants can be found in Ref. 1.

Received 6 July 1999; revision received 12 October 1999; accepted for publication 15 October 1999. Copyright © 1999 by the American Institute of Aeronautics and Astronautics, Inc. All rights reserved.

\*Ph.D. Candidate, Department of Mechanical Engineering, 373-1, Kusong-dong, Yusong-ku.

†Professor, Department of Mechanical Engineering, 373-1, Kusong-dong, Yusong-ku; hjsung@kaist.ac.kr.

## Results and Discussion

It is important to ascertain the accuracy of the present method. Toward this end, an inlet mean velocity profile has been generated by using the present method. The experiment of Vogel and Eaton<sup>4</sup> is employed for comparison, where the flow is over a backward-facing step. Based on the given experimental parameters, that is,  $\delta^*$  and  $\theta$ , a composite velocity profile can be obtained from Eq. (6) in concert with Eqs. (1) and (2). As can be seen in Fig. 1, the mean velocity profile obtained by the present method is reproduced well. In particular, the agreement in the wake region is remarkable. This guarantees the reliability of the present method.

To look into the influence of the inflow condition, three inlet conditions are chosen for comparison. The flow over a backward-facing step is selected as a benchmark test flow. Three inlet conditions are the parabolic profile, the  $\frac{1}{7}$ -power profile, and the present method. The  $k-\varepsilon-f_\mu$  model of Park and Sung<sup>1</sup> is employed as a

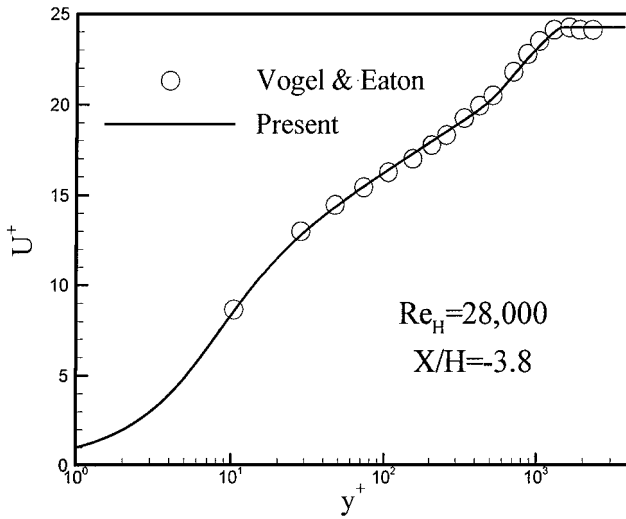


Fig. 1 Comparison of the predicted mean velocity profile with experiment.

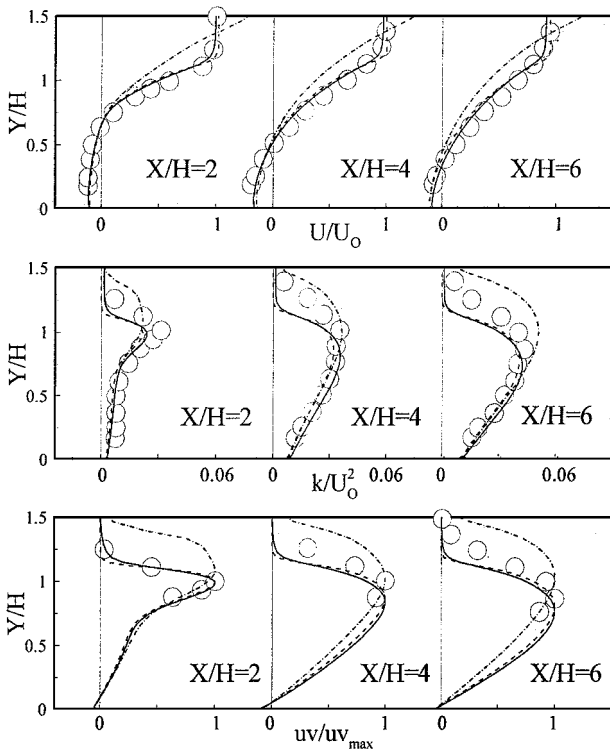


Fig. 2 Comparison of the predicted results by three inlet conditions with experiment for  $U/U_0$ ,  $k/U_0^2$ , and  $\overline{uv}/\overline{uv}_{\max}$ :  $\circ$ , Eaton and Johnston<sup>5</sup>; ---, parabolic; ---,  $\frac{1}{7}$ -power; and —, present.

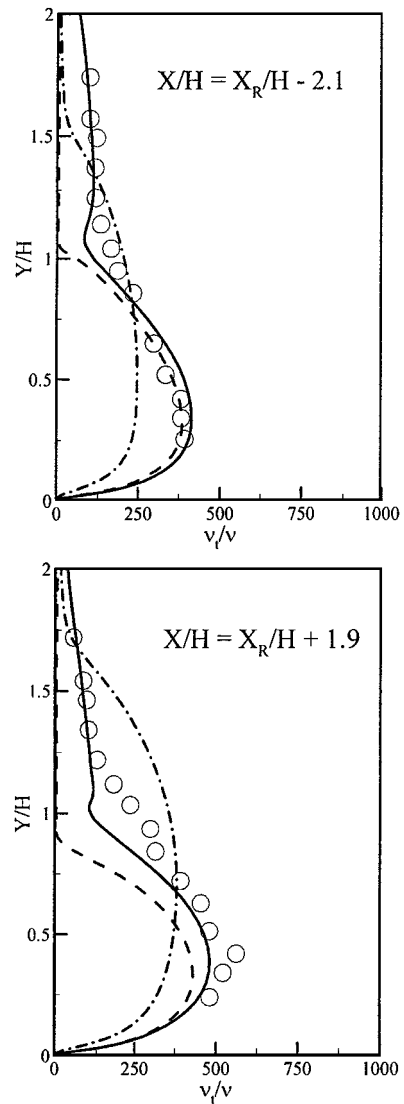


Fig. 3 Comparison of the predicted eddy viscosity with experiment:  $\circ$ , Driver and Seegmiller<sup>6</sup>; ---, parabolic; ---,  $\frac{1}{7}$ -power; and —, present.

RANS closure. In the first two cases, that is, parabolic and  $\frac{1}{7}$ -power, the inlet values of  $k$  and  $\varepsilon$  are given by the formula of Rodi and Scheuerer<sup>7</sup>:  $k = k_e (U/U_e)^2$  and  $\varepsilon = 0.1k(\partial U/\partial y)$ . The predicted results are compared with the experimental data of Eaton and Johnston.<sup>5</sup> As seen in Fig. 2, when the correct inlet profiles are given via the present method, the predicted quantities are in good agreement with the experiment. The predicted results by the  $\frac{1}{7}$ -power profile also give good prediction with a reasonable accuracy. However, the parabolic profile is not a good inflow condition.

The comparison is extended in the distributions of eddy viscosity  $v_t$ , and the results are shown in Fig. 3 for the recirculating region ( $X_R/H - 2.1$ ) as well as for the relaxing region ( $X_R/H + 1.9$ ). Comparisons are made with the experimental data of Driver and Seegmiller.<sup>6</sup> It is encouraging that the results predicted by the present method are in better agreement with the experimental data than those predicted by the  $\frac{1}{7}$ -power profile.

Further evidence by the present method is seen in the comparison of the calculated reattachment lengths  $X_R$  with the experimental results. As seen in Table 1, the computational results obtained by the present method are in excellent agreement with the experiments. Furthermore, the agreement is widely distributed to the ranges, where the adopted experimental conditions cover the ranges  $2.8 \times 10^4 \leq Re_H \leq 3.8 \times 10^4$  and  $1.25 \leq ER \leq 1.667$ , where  $ER$  is the expansion ratio. The reattachment lengths obtained by the  $\frac{1}{7}$ -power law profile are seen to be overpredicted. The degree of overprediction is amplified when the parabolic profile is employed.

Table 1 Comparison of computational reattachment lengths with experiments

Reference	$Re_H \times 10^4$	ER	Results			
			Experiment	Parabolic	$\frac{1}{7}$ -power	Present
Driver and Seegmiller <sup>6</sup>	3.8	1.125	$6.21 \pm 0.2$	10.56	6.85	6.21
Vogel and Eaton <sup>4</sup>	2.8	1.25	$6.65 \pm 0.3$	9.83	7.41	6.59
Eaton and Johnston <sup>5</sup>	3.8	1.667	$7.95 \pm 0.3$	9.47	8.24	7.92

These findings reinforce the ascertainment that the imposition of accurate inlet condition is crucial. It follows that the efforts to test turbulence model performances are far more fruitful when an accurate and robust inlet condition is used.

Conclusions

A simple method for generating inflow conditions for turbulent boundary layers in a RANS closure has been presented. A composite profile was obtained by forming a weighted average of the inner and outer profiles. The mean velocity profile was reproduced well by using the experimental integral parameters. The inflow conditions of  $k$  and  $\varepsilon$  were obtained by solving the  $k-\varepsilon$  equations with the aforestated mean velocity profile. When compared with the computations using other inlet conditions, the proposed method was shown to be highly accurate.

Acknowledgment

This work was supported by a grant from the National Research Laboratory of the Ministry of Science and Technology, Korea.

References

<sup>1</sup>Park, T. S., and Sung, H. J., "A New Low-Reynolds-Number Model for Predictions Involving Multiple Surface," *Fluid Dynamics Research*, Vol. 20,

No. 1, 1997, pp. 97-113.  
<sup>2</sup>White, F. M., *Viscous Fluid Flow*, McGraw-Hill, New York, 1974, pp. 415-420.  
<sup>3</sup>Lund, T. S., Wu, X., and Squires, K. D., "Generation of Turbulent Inflow Data for Spatially-Developing Boundary Layer Simulations," *Journal of Computational Physics*, Vol. 140, No. 2, 1998, pp. 233-258.  
<sup>4</sup>Vogel, J. C., and Eaton, J. K., "Combined Heat Transfer and Fluid Dynamic Measurements Downstream of a Backward-Facing Step," *Journal of Heat and Mass Transfer*, Vol. 107, No. 4, 1985, pp. 922-929.  
<sup>5</sup>Eaton, J. K., and Johnston, J. P., "Turbulent Flow Reattachment: An Experimental Study of the Flow and Structure Behind a Backward-Facing Step," Thermoscience Div., Rept. MD-39, Stanford Univ., Stanford, CA, 1980.  
<sup>6</sup>Driver, D. M., and Seegmiller, H. L., "Features of a Reattaching Turbulent Shear Layer in Divergent Channel Flow," *AIAA Journal*, Vol. 23, No. 2, 1985, pp. 163-171.  
<sup>7</sup>Rodi, W., and Scheuerer, G., "Calculation of Heat Transfer to Convection-Cooled Gas Turbine Blades," *Journal of Engineering for Gas Turbines and Power*, Vol. 107, July 1985, pp. 620-627.  
<sup>8</sup>Parneix, S., Laurence, D., and Durbin, P. A., "A Procedure for Using DNS Databases," *Journal of Fluids Engineering*, Vol. 120, No. 1, 1998, pp. 40-47.

R. M. C. So  
Associate Editor